Control Engineering Practice 145 (2024) 105849

Contents lists available at ScienceDirect

Control Engineering Practice

journal homepage: www.elsevier.com/locate/conengprac

Fuel saving effect and performance of velocity control for modern combustion-powered scooters

Jannis Kreß [a,b,*], Jens Rau [a], Hektor Hebert [a], Fernando Perez-Peña [b], Karsten Schmidt [a], Arturo Morgado-Estévez [b]

[a] Department of Computing and Engineering, Frankfurt University of Applied Sciences, Frankfurt, 60318, Hessen, Germany
[b] Department of Automation, Electronics and Computing Architecture and Networks, University of Cadiz, Puerto Real, 11519, Andalusia, Spain

ARTICLE INFO

Keywords:
Velocity control
Throttle-by-Wire
Fuel saving
Motorcycle powertrain
Alternative restricting

ABSTRACT

This paper investigates the performance and fuel-saving effect of a velocity control algorithm on modern 50 cc scooters (Euro 5). The European Parliament has adopted major CO_2 emission reductions by 2030. But modern combustion-powered scooters are inefficiently restricted and emit unnecessary amounts of CO_2. Replacing the original restriction method with the system presented in this paper, the engine's operating point is being improved significantly. A Throttle-by-Wire-System senses the rider's throttle command and manipulates the throttle valve. A redundant wheel speed sensor measures the precise vehicle velocity using the Hall effect. The entire system is managed by a central ECU, executing the actual velocity control, fail-safe functions, power supply and handling inputs/outputs. For velocity control, an adaptive PI-controller has been simulated, virtually tuned and implemented, limiting the max. velocity regulated by legal constraints (45 km/h). In this way, the environmentally harmful restrictors used today can be bypassed. By implementing a human–machine interface, including a virtual dashboard, the system is capable of interfacing with the rider. For evaluation purposes a measurement box has been developed, logging vehicle orientation, system/control variables and engine parameters. A *Peugeot Kisbee 50 4T* (Euro 5) is serving as test vehicle. Finally, the system has been evaluated regarding performance and fuel efficiency both through simulation and road testing. Fuel savings of 13.6% in real-world test scenarios were achieved while maintaining vehicle performance.

1. Introduction

According to the climate targets of the European Climate Change Act, at least 55% of greenhouse gases are to be saved by 2030 compared to 1990 levels (European Parliament, 2021). Considering the average distance traveled per inhabitant in the EU, the values vary between 5 and 20 km a day. Depending on the country of origin, 57% to 81% is covered by car. Most often, the distance traveled by two-wheelers corresponds to less than 1% (Statistical office of the European Union, 2022). However, for urban mobility, scooters are an excellent alternative. The potential for saving fuel and thus minimizing CO_2 emissions is enormous and can make a significant contribution to EU climate targets. Harmful two-stroke engines are banned and the Euro 5 standard also applies to 50 cc scooters (European Parliament, 2007). Comparing modern four-stroke combustion and electrically powered scooters of Peugeot, Piaggio and Vespa, an average price for electric models of almost 160% can be noticed. These price differences are generally seen for electric vehicles (König et al., 2021). The difference in range is even more striking, as the combustion engine exceeds that of the electric drive by a factor of 6. Users require longer ranges because recharging is often difficult in cities. To fulfill Euro 5 requirements, modern combustion-powered scooters are equipped with gasoline injection and a catalytic converter (Kymco, 2022; Peugeot Motocycle, 2023). To ensure optimal operation of the catalyst, the air/fuel mixture (λ) must be approx. 1 (Görgen et al., 2018). Legal requirements state that 50 cc scooters cannot exceed a maximum speed of 45 km/h. By delaying the ignition timing, the engine is restricted in power, since reducing the fuel injected would cause λ to become larger 1 (lean mixture). This can be solved by deactivating the Original Restriction (OR) of the test vehicle and applying a VC algorithm. The basis is provided by a low-cost TbWS (Kreß et al., 2023), which enables electrical control of the throttle valve. For this purpose, the throttle position is sensed and the throttle valve is manipulated by an actuator. As a consequence, instead of the ignition timing, the airflow is regulated by means of the throttle valve position, which also results in a reduction of the fuel injection volume. This system can contribute substantially to reaching EU climate targets. To the best of our knowledge, this is the first

* Corresponding author at: Department of Computing and Engineering, Frankfurt University of Applied Sciences, Frankfurt, 60318, Hessen, Germany.
E-mail address: jannis.kress@fb2.fra-uas.de (J. Kreß).

https://doi.org/10.1016/j.conengprac.2024.105849
Received 2 November 2023; Received in revised form 23 December 2023; Accepted 10 January 2024
Available online 22 January 2024

approach of a VC application on a modern four-stroke 50 cc (Euro 5) scooter as an alternative restriction. The VC system investigated here is intended to optimize fuel economy and improve exhaust emissions.

1.1. Background on restricting methods

Scooters are defined by EU law. In addition to the max. speed of 45 km/h and the max. engine capacity of 50 cc, the power is also limited to 4 kW, regardless of the type of drive (European Parliament, 2002). In most cases, vehicle performance is sufficient to reach higher speeds, so the surplus power above 45 km/h must be compensated. The surplus is still needed for heavy loads or inclines. In the past, mechanical restrictors were often used, which manipulated the flow behavior either through throttle orifices in the air intake or exhaust (Stoffregen, 2018). Limitation of the Continuously Variable Transmission (CVT) was particularly common, resulting in an unnecessarily high engine speed. Electronic throttling was opened with the arrival of electronic ignition. When the top speed was reached, the ignition was interrupted, resulting in the emission of unburned fuel. Modern powertrains have further capabilities to influence engine control due to gasoline injection. Injection volume and ignition timing are decisive here. Reducing the fuel supplied would be obvious, but leads to high combustion temperatures and interferes with the function of the catalytic converter (Kumar et al., 2023). As a consequence, engine damage and unacceptable exhaust emissions would be expected. Typically, ignition occurs 6° to 40° before the Top Dead Center (TDC), depending on the engine speed. For restriction, the ignition timing is delayed towards the TDC or even behind as shown in Fig. 1 (efficient left, restricted right).

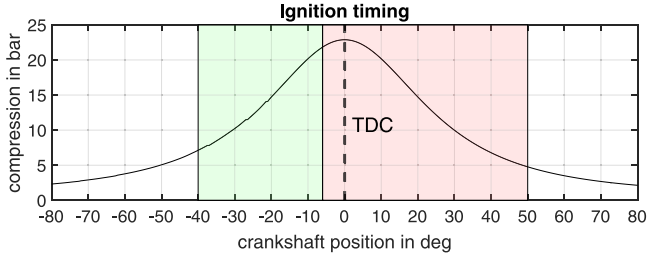

Fig. 1. Ignition timing.

To achieve optimum efficiency, the max. pressure must be reached shortly after TDC. This ensures that the max. combustion chamber pressure can act on the piston from the start of expansion. By retarding the ignition timing, expansion is already taking place during combustion, thus reducing both the peak pressure and the usable expansion distance. The efficiency drops (Leyda & Wos, 2012).

1.2. Background on TbWSs

TbWSs have been researched and integrated industrially to motorcycles (Corno et al., 2008; Miritsch et al., 2021; Poschner et al., 2010). A TbWS has also been applied successfully to small-volume engines, coming with the minimum number of low-cost components, combined in the throttle body. The system is based on a throttle servo, throttle position sensor, throttle demand and speed sensor. To limit and adapt the engine speed in various load situations, the speed can be adjusted by an integral electronic control and resonant frequencies can be avoided. Besides the performance limitation, the system is capable of managing speed and load reductions during overheating. For cold starts, the idle speed can be adjusted on the outside temperature (Smither et al., 2008). Also, an electronic throttle control (ETC) for a 50 cc two-stroke scooter application has been developed, improving fuel economy, idle-stability and implementing an electronic vehicle velocity limitation. By use of an electronic throttle control, the conventional CVT restriction can be replaced, which leads to fuel savings of 22% caused by the lowered engine speed. Additionally, the system allows controlling the idle engine speed after the start-up. The system is based on a carburetor-driven two-stroke scooter with a power of 4.2 kW and a twin variator pulley CVT (Smither et al., 2011). Due to the mentioned powertrain, the system is not compliant with the Euro 5 standard. Nowadays systems use an originally optimal-designed CVT. In addition, modern air-cooled four-strokes have a power output of max. 2.5 kW due to the lower power density. The potential within power surplus and transmission thus no longer exists. In addition, the fuel consumption of modern non-optimized scooter drives is considerably lower than that of an optimized two-stroke (Zhang & Zhao, 2014).

For restricting modern combustion-powered 50 cc scooters, the state of the art is represented by Ignition Timing Manipulation (ITM). Mechanical restrictions such as orifices, throttle stops or CVT limitations are rarely used anymore due to significant performance losses and high powertrain stresses. Ignition interruption would lead to strong vibrations in single-cylinder four-stroke engines and were used primarily on two-stroke engines. Since modern scooters are equipped with a three-way catalytic converter, the restriction must not have any influence on the oxygen concentration in the exhaust gas, as otherwise the degree of conversion will be affected. The presented TbWSs improve engine control at different load points/influences or lead to fuel savings when mechanical restrictions are removed. Due to the optimized gear ratios and the elimination of mechanical restrictions, no increase in efficiency would be expected. Table 1 points out the VC's main contribution by listing its advantages in contrast to ITM.

Table 1
List of contribution.

Restriction	ITM	VC
Method	Shift ignition timing	Control air supply
Ign. tim. (v_{max})	−11.5 degree to TDC	−32 degree to TCD
Effect	Combust. in exhaust	Efficient combust.
Throttle opening	100%	50%
Fuel inj. (v_{max})	100%	75%
Fuel economy	2.11 l/100 km	1.82 l/100 km
Performance	100%	100%
Precision	± 0.3 km/h	± 0 km/h

2. System development

The TbW-based VC uses the set velocity (throttle grip position) specified by the rider as the command variable/input. A WSS measures the vehicle's dynamics (velocity), used as control reference variable. Driving mode and settings serve as additional rider input. The desired vehicle velocity is manipulated through an electronically set throttle valve position (output). For safety reasons, the system is capable of interrupting the engine's ignition line. Lastly, the system requires power supply, outputs diagnose data and rider-intended system information for evaluation purposes. Fig. 2 shows a general black box schematic.

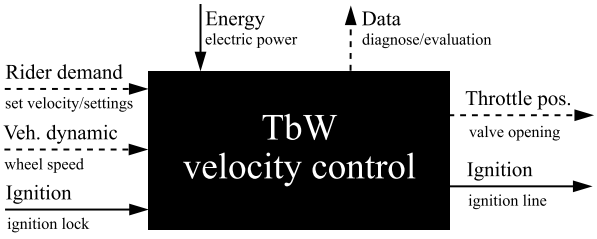

Fig. 2. Blackbox schematic.

Several bus-connected subsystems are required to implement VC and efficient restriction. The sensing of the rider's demand (throttle grip position) and the vehicle velocity must be achieved. To be able to influence the scooter's longitudinal driving dynamics, the throttle valve position must be controlled electronically. In parallel, emulation of the Engine Controller (EC) is essential to prevent ITM. The remaining drive-train, consisting of the engine, gearbox and rear wheel, retains its original condition. A central Main Electronic Control Unit (MECU) processes input variables, performs VC, provides necessary data on the bus and ensures safe vehicle operation. Furthermore, the MECU

serves as power box, providing electric energy to all subsystems. The overall system shall be designed in such way, as to allow switching between restrictions by ITM and throttle valve manipulation. By means of a virtual dashboard, system quantities and an eco-score are to be displayed to the rider. For evaluation, this HMI will be used to switch between restrictions and to start measurements. These are to be recorded by a Measurement Box (MB) accessing the vehicle bus. Now that the foundation has been laid for assistance systems, cruise control is to be implemented. This section presents the architecture developed, including the sensors and systems needed. Fig. 3 gives the system layout which has been outlined. Table 2 lists required quantities related to the system development.

Table 2
List of quantities.

	Quantity	Symbol	Value/unit
1	Air density	ρ	1.225 kg/m^3
2	Array size	s_A	–
3	Clutch bell poles	n_{poles}	4
4	Control deviation	dev	km/h
5	Force, Air resistance	F_{Air}	N
6	Force, Drive	F_{Drive}	N
7	Force, Rolling resistance	F_{Roll}	N
8	Force, rotational inertia	$F_{I_{rot}}$	N
9	Force, translational inertia	$F_{I_{trans}}$	N
10	Frontal area	A	0.78 m^2
11	Gain, integral	K_I	–
12	Gain, proportional	K_P	–
13	Gain, threshold	K_T	–
14	Inertia front wheel	J_f	0.327 Nms^2
15	Inertia rear wheel	J_r	1.323 Nms^2
16	Integral enable flag	I_{enbl}	{0, 1}
17	Integral offset	Os	3.0 km/h
18	Integral threshold	T_I	–
19	Mass rider	m_r	80 kg
20	Mass scooter	m_{sc}	99 kg
21	Resistance, air coefficient	c_w	0.64
22	Resistance, rolling coefficient	c_r	0.015
23	Scooter velocity	v_{sc}	km/h
24	Top speed	v_{max}	48.7 km/h
25	Throttle valve position	Pos_{thr}	%
26	Time per step	t_{step}	s
27	Transmission ratio	i_{gear}	13
28	Wheel diameter	D_{Wheel}	1.42 m
29	Wheel radius	r	0.226 m
30	WSS, period time	T_{WSS}	s
31	WSS, step distance	d_{step}	m
32	WSS, number of steps	n_{steps}	48

2.1. Throttle-by-Wire-System

The basis for the VC implementation is provided by the previously developed low-cost TbWS. A redundant, contactless AMR sensor is used to sense the throttle position with a measuring accuracy of 99.84%. The measured and plausibility-checked position is sent via CAN by the Throttle Position Sensor (TPS). To enable the system's influence onto longitudinal vehicle dynamics, a Throttle Valve Actuator (TVA) was developed. By determining the position using a Hall sensor in combination with a stepper motor, the throttle valve can be precisely position-controlled. This allows positioning with an accuracy of 99.63% within max. 60 ms. TPS and TVA make use of embedded fail-safe functions, monitoring measurement and position quality. Design, function, reliability and performance have been evaluated (Kreß et al., 2023).

2.2. Wheel speed sensor

The scooter's velocity is required as a control variable for VC. Since 50 cc scooters are not legally obligated to be equipped with an anti-lock braking system, they do not have WSSs (European Parliament, 2013). In the test vehicle, the rear wheel speed is only measured with a passive inductive Transmission Speed Sensor (TSS) on the clutch bell for restriction. Due to its design, it is not suitable for measuring low speeds. Therefore, a redundant WSS was developed, which enables the precise sensing of the wheel speed, as shown in Fig. 4.

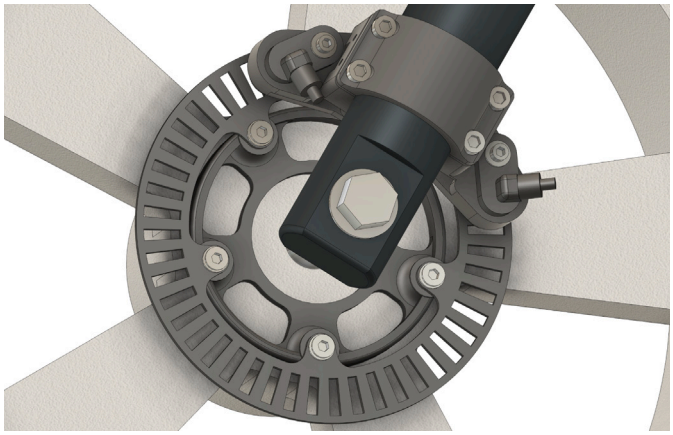

Fig. 4. WSS adaption.

Two automotive magnetostatic WSSs independently measure the motion of a 48-step encoder disc by determining the width of successive pulses. A sampling rate of 1 MHz results in a resolution of 0.02 km/h. The WSS assembly was tested within a hardware-in-the-loop environment (Kreß et al., 2021). The assembly is to be integrated, whereby a constant distance (<0.5 mm) between sensors and the encoder disc is to be ensured. Preferably, the controlled rear wheel speed is sensed to intervene in case of wheel slip. Adaptations were developed in several iterations. Unlike chain-driven motorcycles, there is no decoupling between the driven wheel and the engine/gearbox. Vibrations from strong low to high frequencies are directly transferred to the WSS resulting in extreme measurement inaccuracies. Decoupling, damping and software filters for signal processing could not achieve sufficient signal quality. For that reason, the WSS is adapted to the front wheel. In addition, the TSS is used to detect wheel slip/lock at the rear. With a bracket, both sensors are precisely placed.

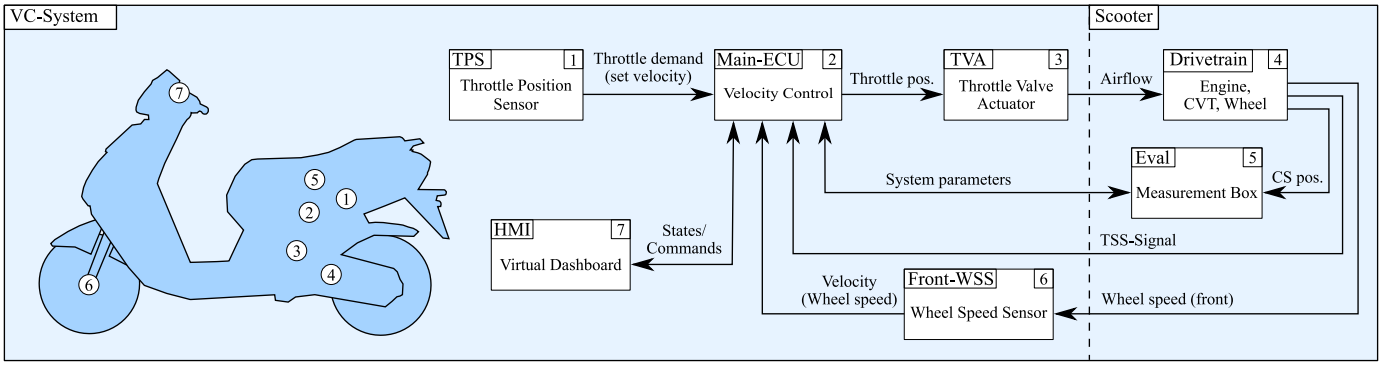

Fig. 3. System layout.

2.3. Main Electronic Control Unit

The Main Electronic Control Unit (*STM32G431KB*) (STMicroelectronics, 2021) is intended to act as a higher-level system master. On the input side, this includes processing the wheel speed, receiving the TPS measured value and the rider command from the HMI. On the output side, the TVA position, HMI system states, emulated TSS signal and evaluation data must be transmitted. At the hardware level, the MECU must supply the entire system with power, provide the measurement electronics of the WSSs and enable the amplification of the emulated speed signal. At software level, the VC needs to be implemented, adjusting the vehicle's velocity to the rider's demand. Here, the continuous functional safety of the overall system must be ensured by means of appropriate fail-safe functions.

Power box: The MECU provides individually fused voltages to all subsystems. Especially the TVA motor is to be supplied with an independent power line to prevent system errors in case of damage. Three 12 V DC/DC step-down converters provide stabilized voltages of 3.3 V (MECU internal), 6 V (TVA motor) and 7.5 V (common system voltage). In addition, the 12 V battery voltage is also provided. A wiring harness originates from the MECU that connects all subsystems, consisting of 6 wires: GND, VCC_{step}, VCC_{sys}, VCC_{bat}, CAN_H and CAN_L.

WSS processing: A square-wave signal voltage is generated via a measuring resistor in the supply line of the WSSs. The signal conversion must be performed by the MECU for the WSS (front) and TSS (rear). The WSS signal acquisition can be done by external interrupts due to the constant measuring voltage. For processing the TSS, a comparator is used to digitize the varying voltage of the inductive sensor. Afterward, the given pulse widths are measured by an input capture timer. The stored pulse widths (T_{wss}) are smoothed by a moving average filter with the array size of (s_A) before velocity conversion (v_{sc}). For the determination, the wheel circumference (D_{wheel}) and the resolution of the encoder disc (n_{steps}) are required. Eq. (1) transfers the pulse widths into a velocity. In order to prevent dead time behavior, the WSS's array size (s_A) adapts to vehicle velocity. Due to the redundant signals, errors in velocity measurement can be detected.

$$v_{sc} = \frac{d_{step}}{t_{step}} = \frac{D_{wheel}}{n_{steps}} \cdot \frac{s_A}{\sum_0^{s_A} T_{wss}} \tag{1}$$

Sensor emulation: For bypassing the OR, the original EC needs to be emulated with a manipulated TSS signal. Therefore, a signal is to be emulated and amplified, depending on the current velocity (v_{sc}). The output frequency chosen is two times lower than the oscillating signal provided by the TSS. That way, the EC is not interfering the optimal ignition timing. For proper stimulation, the emulated signal has to be within the original speed-dependent voltage range (±30 V). The emulated signal is generated by switching the 12 V battery voltage by a MOSFET, overcoming the ECs threshold. Eq. (2) is used to calculate the emulating frequency (f_{emul}) for the PWM timer, based on the second-stage transmission ratio ($i_{gear} = 13$) and the number of poles ($n_{pole} = 4$) attached to the clutch bell. For a velocity of max. 50 km/h, a frequency of 3.64 kHz results. To facilitate the comparison between the OR and VC system, a switch can be used to select between transferring the emulated or original TSS signal to the EC.

$$f_{emul}(v_{sc}) = v_{sc} \cdot \frac{2 \cdot i_{gear} \cdot n_{pole}}{D_{wheel}} \tag{2}$$

Fail-safe: Every system interfering with vehicle dynamics, is to be classified as safety critical. The system manipulates longitudinal dynamics by throttle intervention. Depending on the error detected, the MECU must react by predefined fail-safe states to ensure safe vehicle operation. Table 3 shows the error cases identified as possible. The listed fail-safe states are classified into four stages. Class 1 describes warnings that require re-calibration but do not danger safe operation. Class 2 can affect the operation by malfunction of the cruise control, which is why it is disabled. Class 3 can lead to total scooter misbehavior by loss of acceleration control. In this case, the TVA is not accepting any throttle request. Class 4 represents the worst case. The MECU can no longer control the powertrain and a contactor interrupts the ignition line to shut down the engine. A relay is to be integrated, controlling the ignition line. All error cases include monitoring of CAN communication, using safety features like counters and CRC.

Table 3
List of fail-safe states.

ID	C	Error	Type	Action
1	1	TPS calib. required	Warning	HMI notification
2	1	TVA calib. required	Warning	HMI notification
3	2	HMI CAN error	Error	Disable cruise control
4	3	WSS inaccuracy	Error	Reset TVA & set velocity
5	3	TPS error detected	Error	Reset TVA & set velocity
6	4	TVA error detected	Error	Engine shut down

2.4. Velocity control

Conventional vehicles require a throttle command by the rider that relates to the required power needed. The rider controls the desired vehicle velocity. The VC approach describes a continuous control of the velocity. Instead of any required engine power, the throttle grip position represents a set velocity. Basically, the system performs a continuously varying cruise control algorithm. For this, a controller is designed, as shown in Fig. 5. The TPS set velocity (w_θ) serves as input reference variable. After determining the control deviation (e_θ) by using the WSS measurement as control variable feedback (y_{θ_meas}), the PI-controller outputs the manipulated variable u_ω in form of a throttle valve opening. Next, the TVA controls the airflow ($u_{A\theta}$) within the air intake. Then, the powertrain reacts to the system's throttle demand and generates a propulsion force in relation to the throttle valve opening. Windy conditions, heavy load or street gradients can result in a disturbing/varying resistance force (F_{resist}). The vehicle velocity y_θ is measured by the WSS and fed back.

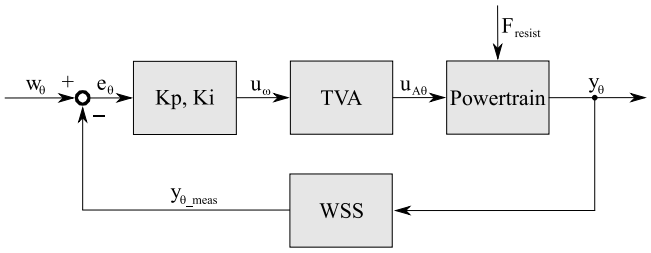

Fig. 5. VC control loop.

Modeling: For adequate controller design, the system is simulated. Considering translatory ($F_{I_{trans}}$) and rotational ($F_{I_{rot}}$) mass inertia, air (F_{Air}) and rolling (F_{Roll}) resistance, the equilibrium of forces is described in (3).

$$F_{Drive} = F_{I_{trans}} + F_{I_{rot}} + F_{Air} + F_{Roll} \tag{3}$$

In dependence on the vehicle position, a non-linear differential equation of second-order results for F_{Drive} in (4). The constants were measured or determined experimentally and are listed in Table 2.

$$F_{Drive}(x) = (m_{sc} + m_r) \cdot \ddot{x} + \frac{(J_f + J_r)}{r^2} \cdot \ddot{x} + \frac{A \cdot \rho \cdot c_w}{2} \cdot \dot{x}^2 + c_r \cdot (m_{sc} + m_r) \cdot g \tag{4}$$

F_{drive} depends on the operating point of the engine and gearbox. To determine the power characteristics, performance measurements were taken on a roller dynamometer at various operating points, shown in Fig. 6. With the clutch engagement, the power increases up to 15 km/h. The power declines with growing velocity due to the poor CVT efficiency and the speed-dependent power drop of the engine. Caused by the test setup, the F_{Roll} is part of the measured power and has to be compensated proportionally in case of partial load conditions.

A polynomial ($P(v)_{poly}$) is derived from the data set. For a full throttle acceleration, the driving force can be determined by (5).

$$F_{Drive}(\dot{x}) = \frac{P(v)_{poly}}{\dot{x}} \tag{5}$$

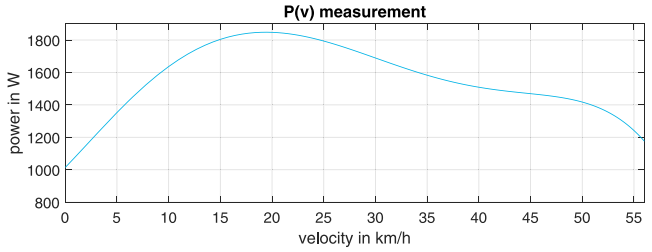

Fig. 6. Engine characteristics.

To check on model plausibility, the simulated step response was compared to a reference measurement, shown in Fig. 7. The final velocities and the acceleration behavior match. The maximum deviation is ±1 km/h and the validity of the simulation is sufficient. In addition, the simulated forces are shown as further simulation output.

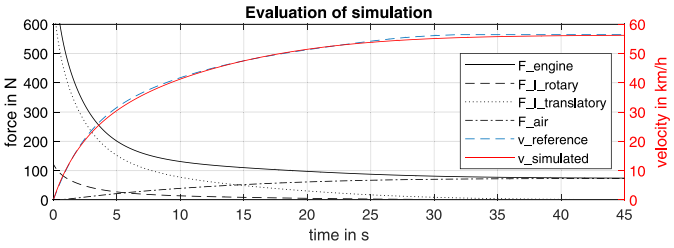

Fig. 7. Evaluation of simulation.

Control: By applying the VC, the throttle grip position equals a set velocity. Controlling the scooter's velocity constitutes a non-linear system. With increasing velocity, the control deviation rises due to higher driving resistance. Typically, control algorithms for non-linear systems are optimized for a certain operating point by linearization. Here, an adaptive PI-controller is proposed to change its characteristics velocity-dependent. This strategy achieves a balance between high controllability and control accuracy over the whole velocity range. In theory, a P-controller could already lead to adequate control behavior. If the gain is too high, not only the overshoot behavior but also signal disturbances of the velocity feedback would negatively affect the performance. Through adding an I-controller, the set velocity can be reached by smaller P-gains, stabilizing the controller and decreasing the susceptibility to disturbances. Therefore, the controller's parametrization needs to adapt continuously to the scooter's operating point. Proportional (K_P) and integral (K_I) gain adapts to the current scooter velocity (v_{sc}) given in (6) and (7). For both, the max./min. gain is to be determined. A constant 3.0 km/h offset (Os) of the linear I gain curve prevents instability at very low velocities.

$$K_P = \frac{v_{sc}}{v_{max}} \cdot (K_{P_{max}} - K_{P_{min}}) + K_{P_{min}} \tag{6}$$

$$K_I = \frac{v_{sc} - Os}{v_{max}} \cdot (K_{I_{max}} - K_{I_{min}}) + K_{I_{min}} \tag{7}$$

Caused by the continuously changing set velocity and the varying steps within the throttle command, the I-controller cannot perform precisely. Depending on the operating point, there are different settling times for different velocities and, as a result, varying integral values/overshoots. By implementing a set velocity-dependent threshold (T_I), the enabling time of the I-controller can be predefined related to the rising control deviation (dev) and set velocity (v_{set}). T_I is described by (8).

$$T_I = \frac{v_{set}}{v_{max}} \cdot (K_{T_{max}} - K_{T_{min}}) + K_{T_{min}} \tag{8}$$

If the control deviation overcomes the threshold in its current operating point, the integrator is reset and disabled by (9). The I-controller is only enabled in a certain error band in order to adjust the system as precisely as possible. This error band is centered around the set point and changes its size relative to the set point. This allows the control behavior to be kept consistent, regardless of the operating point and abrupt throttle commands. Additionally, the integrator is limited to prevent an integration wind-up when the actuator is saturated.

$$(dev > T_I) \quad I_{enbl} = 0 \quad ; \quad (dev \leq T_I) \quad I_{enbl} = 1 \tag{9}$$

The throttle valve position (Pos_{thr}) is given by (10).

$$Pos_{thr} = K_P(v_{sc}) \cdot dev + K_I(v_{sc}) \cdot I_{enbl}(T_I) \cdot \int dev \tag{10}$$

Based on the longitudinal scooter model, a closed loop simulation was set up for tuning the controller. A max. overshoot of 0.3 km/h (barely noticeable for the rider) and robust control behavior, under consideration of sensor disturbances, were required. In addition to a fast settling time, driveability was also taken into account. At high gains, the powertrain reacts too sensitively to small throttle deflections, despite constantly stable control behavior. Therefore, a parameter set was chosen that combines the highest possible performance with enabling smooth accelerations. Using simulation, it was determined which parameter set was best with regard to control performance. This was then optimized for driveability in a road test. Table 4 shows the resulting controller parameters. The algorithm is being executed with a cycle time of 20 ms.

Table 4
List of controller parameters.

	P	I_{sim}	I	$T_{I,sim}$	T_I
K_{min}	2.1	0.02	0.01	1.44	1.3
K_{max}	16	0.07	0.075	6.84	6.3
Os	/	3.0	3.0	3.0	3.0
Limit (%)	−100/100	0/100	0/100	0/100	0/100

2.5. HMI - virtual dashboard

Virtual dashboards are uncommon in this vehicle class. In context of the VC, cruise control and driving modes, they offer plenty of opportunities for adequate visualization and interaction. The HMI consists of a 4.3″ LCD display combined with a STM32 MCU (H7B3) (STMicroelectronics, 2019). Inputs were realized using a micro joystick integrated into the throttle armature. In addition to the original information, the following functions have been enhanced, as shown in Fig. 8.

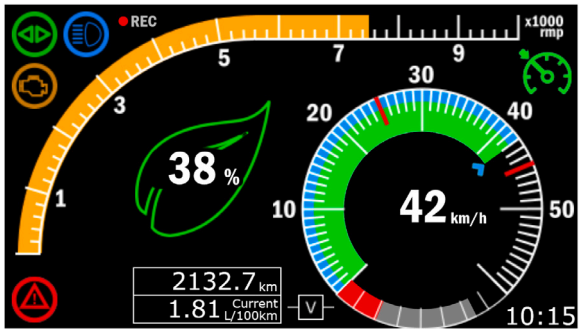

Fig. 8. HMI virtual dashboard.

1. Set/scooter velocity: Based on the VC strategy, the velocity demand (blue, outer radius) given by the rider needs to be displayed in addition to the scooter velocity (green, inner radius).
2. Cruise control interface: For enabling/disabling the cruise control, the selected velocity is set by a small arrow in combination with a cruise control sign.
3. Eco-score: To encourage eco-friendly driving, an eco-score (green leaf) is built up with fuel savings made.
4. Evaluation information: The engine speed, amount of fuel injected and recording state of the MB are to be displayed.

5. Driving mode: By use of the HMI, the developer can switch between the OR (TSS signal/no VC) and enabled VC-System (TSS emulated by MECU).

2.6. Measurement box

For system integration, VC parametrization and lastly functional verification, system states and dynamic vehicle data must be measured. Therefore, a MB was designed for logging CAN bus data, measuring engine speed and injection cycle, storing files in real-time and offering data transfer via a microSD card. Set point and process value of the velocity as well as the throttle valve position are tapped directly from the vehicle's CAN bus. For the measurement of the current engine speed, the speed signal of the original crankshaft sensor was processed and evaluated. To measure vehicle dynamics, a 6-axis inertial measurement unit was used, fusing sensor values by complementary filters to measure orientation and acceleration. All measured quantities are periodically stored with a time stamp, provided by a real-time clock. As shown in Fig. 3, the MB (No. 5) is not part of the VC-system. Starting or stopping a recording is done via the HMI. New files are automatically created and adjustments to the recording rate or CAN message selection can be edited quickly.

3. Results

The VC is investigated in terms of control performance, system behavior in various scenarios and fuel economy.

3.1. Control performance

To achieve stable, stationary and precise control, an adaptive PI-controller was tuned simulation-based (Table 4) under the criteria of max. 0.3 km/h overshoot. A test cycle, consisting of a series of increasing velocity steps (0, 10, 20, … km/h) and sudden accelerations from standstill (0, 10, 0, 20, … km/h), was performed. The set values were provided by the implemented cruise control in order to achieve optimum reproducibility. That way, the proper function of the adaptive threshold for larger steps in set point as well as small variations can be tested. By comparing the set velocity with the resulting simulated/measured velocity and the simulated closed-loop/measured TVA position, the simulation validity and real-world control performance can be investigated. Fig. 9 presents the test results (top: incremental, bottom: initial).

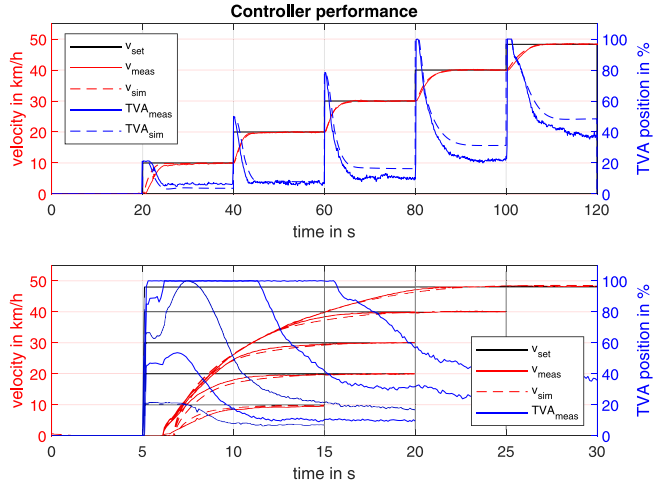

Fig. 9. Controller performance.

For both scenarios, the controller reached the exact set velocity without any overshoot or instability. Velocities lower than 11 km/h led to unsteady settling due to the centrifugal clutch engagement/slip. For higher velocities, the max. error between simulated and measured dynamics is 1.9% for step-wise increments. Initial accelerations from standstill lead to shifted velocity origins that can be justified by the clutch engagement. The resulting error is max. 2.3% which proves a plausible controller simulation beyond the engagement process. Deviations in TVA openings are due to the non-linear relationship between throttle opening and engine power output. This was neglected in the simulation, but has no measurable effect on the control behavior. Higher controller gains are feasible but lead to oversensitive response to throttle changes. Fig. 9 also demonstrates the proper operation of the cruise control.

3.2. System behavior

After validation of the control strategy and performance, the effect on vehicle dynamics and engine control is to be examined in real-world scenarios. Three frequently occurring disturbance scenarios were analyzed: max. acceleration (S1), a sudden change from a level road to an uphill/downhill slope (S2) and an acceleration on a downward slope followed by a transition to a level (S3). The comparison to the OR is shown in Fig. 10 by measurements of the velocity, throttle valve position and the fuel injected. Differences between scenarios result from small road gradient variations.

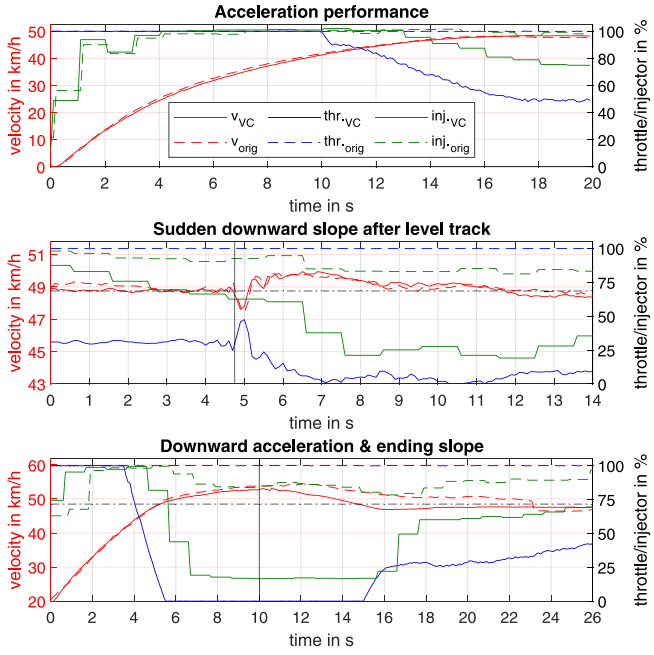

Fig. 10. System behavior.

Scenario (S1) demonstrates the preservation of driving performance. Acceleration is equally fast with both systems, whereby the OR, contrary to the VC, shows a slight overshoot of 0.3 km/h (VC: 0 km/h) when reaching the speed limit. Significant differences can be found in the throttle valve position and injection quantity. When approaching the speed limit (orig. 48.7 km/h, dash-dotted line), the VC regulates the throttle valve at the corresponding operating point (50%). Consequently, the injection quantity also drops by 25%. Scenario (S2) is initiated at top speed, which is why the VC has already settled to approx. 35% throttle position. At time 4.75 s, an 8% downhill slope suddenly occurs after a small bump. Despite aggressive excitation, the system behavior remains stable and even resembles the response of the control applied by Peugeot. In both cases, the overshoot behavior at the entry of the gradient also shows max. 1 km/h. The VC closes the throttle valve almost completely, whereas originally it is fully open and three times the fuel is injected. Scenario (S3) shows the max. acceleration on a 15% downhill slope followed by a transition to level ground. An improved overshoot (1.1 km/h smaller) can be seen with the VC. While the speed limit can no longer be maintained with OR, it can be

successfully controlled by the VC. It is shown again that the throttle valve is completely closed and the injection is reduced to idle state. At time 10 s, the gradient ends. The system response is stable with no discernible fluctuations in velocity.

3.3. Fuel savings

In order to demonstrate the fuel savings/CO_2 reduction under real-world conditions, a 50.4 km long test cycle was driven that depicts 61% urban and 39% rural environments. Three cycles each were driven for the OR and the VC-system. Weather conditions, driving time and traffic situation were monitored to create comparable test conditions. The tire pressure was kept constant at the manufacturer's specification of 2.1 bar and the rider (85 kg) was not changed. Consumptions were determined by means of calibrated measuring cylinders. Inaccuracies of max. 2.5 ml occur due to measurement errors, which result in a max. total error of 0.3%. The measured volumes were referenced to a temperature of +15 °C. By applying the VC, a saving of 13.6% (1.82 l/100 km) could be demonstrated compared to the OR (2.11 l/100 km). Since the combustion of one liter of gasoline releases 2280 g CO_2, this corresponds to an estimated reduction of approx. 661 g/100 km. Table 5 shows the related results.

Table 5
List of Road testing results.

Mod.	Weath. °C	Dur. h	Mile. km	Vol. ml	Cons. $\frac{l}{100\ km}$	Aver. $\frac{l}{100\ km}$
Orig.	sun,dry,12	1:25	50.4	1060	2.10	
Orig.	sun,dry,16	1:26	50.4	1061	2.10	**2.11**
Orig.	sun,dry,17	1:31	50.4	1065	2.11	
VC	sun,dry,17	1:29	50.4	925	1.83	
VC	sun,dry,12	1:32	50.4	885	1.76	**1.82**
VC	sun,dry,18	1:33	50.4	945	1.87	

This saving can be explained by the optimization of the ignition timing. On the flat, approx. −11.5 degrees before the TDC can be measured with OR. By applying the TbWS, the air supply is controlled instead of the ignition timing. This allows the EC to set the optimum ignition timing and reduce the injection quantity to maintain $\lambda = 1$. Now the ignition timing corresponds to −32 degrees at max. velocity and is thus in the optimum range (compare Fig. 1). A significant improvement in exhaust gas composition can also be expected.

4. Discussion

Modern four-stroke scooters already enable a comparatively environmentally friendly type of individual mobility. The system developed increases efficiency by an additional 14%. More and more electric scooters are available as alternatives, but they come with significantly smaller ranges, heavy batteries and higher prices. If CO_2 emissions are considered in comparison, vehicle production and electricity generation must be considered. One liter of gasoline emits about 2280 g (Kawamoto et al., 2019) of CO_2 when burned, while the European average for the production of one kilowatt-hour of electrical energy is about 226 g of $C0_2$ (World Energy Council, 2021). The average consumption of combustion-powered scooters from several leading manufacturers in the EU (Peugeot, Vespa, Piaggio) equals an average of 2.22 l/100 km (5143 gCO_2/100 km) for gasoline-powered and 4.11 kWh/100 km (928 gCO_2/100 km) for electric-powered scooters. Taking into account the average battery capacity of the referred manufacturers, a capacity of 4.88 kWh results. The production emissions of both vehicle types differ mainly through battery production, which releases about 177 kg of CO_2 per kWh of capacity (Kawamoto et al., 2019). Consequently, the electric drive generates an additional 864 kg offset of CO_2 on average. With a life expectancy of scooters/mopeds of 20 000 km, the CO_2 emission for the gasoline-powered scooter is 1028.6 kg and 1049.6 kg for the electric-powered one. The test vehicle equipped with the velocity-controlled TbWS achieves a CO_2 footprint of 829.9 kg during its service life with an average consumption of 1.81 l/100 km, making it 20.9% more environmentally friendly than average electric scooters. After 26 800 km, the electric scooter would show a CO_2 benefit. When charging with electricity from renewable energy sources solely, the emissions caused by battery production would still overcome the test vehicle's footprint. By using eco-fuels, the CO_2 balance could even be neutral. Accordingly, consumption optimization would serve for economic efficiency and effective utilization of the eco-fuel resource (Agarwal & Valera, 2022).

Besides the eco-friendliness, the driving experience can be questioned. By VC implementation, there is no direct command line to the engine. The system reacts proportionally to the control deviation, which is similar to conventional acceleration behavior. Like cruise control, the system can accelerate independently on uphill/downhill grades to maintain speed. The rider has to get used to this behavior, as it differs from conventional scooters. Other control approaches could be considered. Furthermore, the highest energy loss of 28% (test vehicle) occurs in the variomatic transmission. This design-related problem affects all scooters with CVT belt drive (Zhu et al., 2010). In future, the development of a more efficient torque converter could increase the fuel economy. Consumption of less than 1.5 l/100 km could become feasible. Hydrodynamic torque converters could be investigated (Lindemann et al., 2014).

Finally, the question of system costs arises when it comes to integration in cost-effective scooters. Previous research has estimated the costs for the TbWS at approx. 15 € for large-scale production (Kreß et al., 2023). Components such as the MB or the virtual dashboard are not required for VC implementation. MECU and WSS, in contrast, must be considered. Prototype costs amount to approx. 35 € for the MECU and approx. 60 € for the WSS. Taking into account discounted purchase prices, high quantities and mass production, experience has shown a fall to almost 10% of the initial costs. The system costs would be estimated to 25-35 €. Further, the merging of MECU, TPS and TVA electronics into a fully integrated unit offers additional potential for cost savings.

5. Conclusion

In this article, the development of a velocity-controlled Throttle-by-Wire-System is presented. The objective, to provide a more eco-friendly restriction method, was successfully reached. Instead of shifting the ignition timing to comply with the legal maximum velocity for scooters, this system regulates the air supply to the engine. For this purpose, a wheel speed and throttle grip sensor were designed to sense feedback and control variable. A throttle actuator was designed to allow system intervention by engine power manipulation. Power supply, data processing, motor control emulation, fail-safe functions and actual control were implemented on a Main Electronic Control Unit. By simulating the vehicle's longitudinal dynamics, an adaptive controller could be designed to control the velocity stable, with stationary accuracy and without overshoot. Control of the vehicle's top speed has been improved in terms of accuracy and overshoot. The driveability/operability of the vehicle was prioritized. A virtual dashboard was used to interface between the system and the rider, clarifying the functionality and promoting eco-friendly driving with an eco-score. Additionally, it enables the activation and adjustment of the cruise control. In order to be able to evaluate the system behavior, a measurement box was integrated, logging all system parameters. Ultimately, a fuel saving of 13.6% was achieved and proven in the road test, while maintaining the vehicle's performance. These savings are caused by the prevention of ignition timing manipulation for restriction. As a result, the competitiveness against electrically powered scooters/mopeds was underlined. As long as large amounts of CO_2 are emitted during battery production, the optimized four-stroke powertrain presented here represents an excellent transitional solution. Mechanical optimizations could further reduce consumption.

CRediT authorship contribution statement

Jannis Kreß: Conceptualization, Data curation, Formal analysis, Funding acquisition, Investigation, Methodology, Project administration, Resources, Software, Supervision, Validation, Visualization, Writing – original draft, Writing – review & editing. **Jens Rau:** Software, Validation, Visualization, Writing – review & editing. **Hektor Hebert:** Project administration, Supervision. **Fernando Perez-Peña:** Supervision, Writing – review & editing. **Karsten Schmidt:** Writing – review & editing. **Arturo Morgado-Estévez:** Project administration, Supervision, Writing – review & editing.

Declaration of competing interest

The authors declare that they have no known competing financial interests or personal relationships that could have appeared to influence the work reported in this paper.

Acknowledgments

The herein presented research was funded and supported by the University of Cadiz, Spain and Frankfurt University of Applied Sciences, Germany. The authors acknowledge the valuable support of Peugeot Motocycles Deutschland GmbH.

Appendix A. Supplementary data

Supplementary material related to this article can be found online at https://doi.org/10.1016/j.conengprac.2024.105849.

References

Agarwal, A. K., & Valera, H. (2022). *Greener and scalable E-fuels for decarbonization of transport* (1st ed.). (p. 3). Singapore: Springer Singapore, http://dx.doi.org/10.1007/978-981-16-8344-2.

Corno, M., Ranelli, M., Savaresi, S. M., Fabbri, L., & Nardo, L. (2008). Electronic throttle control for ride-by-wire in sport motorcycles. In *Proc. 17th IEEE international conference on control applications* (pp. 223–238). http://dx.doi.org/10.1109/CCA.2008.4629640.

European Parliament (2002). Directive 2002/24/EC relating to the type-approval of two or three-wheel motor vehicles and repealing council directive 92/61/EEC. *Official Journal of the European Communities*, *2002/24/EC*.

European Parliament (2007). Regulation on type approval of motor vehicles with respect to emissions from light passenger and commercial vehicles (Euro 5 and Euro 6) and on access to vehicle repair and maintenance information. *Official Journal of the European Union*, *No 715/2007*.

European Parliament (2013). Regulation on the approval and market surveillance of two- or three-wheel vehicles and quadricycles. *Official Journal of the European Union*, *No 168/2013*.

European Parliament (2021). Establishing the framework for achieving climate neutrality and amending regulations ('European climate law'). *Official Journal of the European Union*, *(EC) No 401/2009 and (EU) 2018/1999*.

Görgen, M., Balazs, A., Böhmer, M., Nijs, M., Lehn, H., Scharf, J., Thewes, M., Müller, A., Alt, N., Claßen, J., & Sterlepper, S. (2018). All lambda 1 gasoline powertrains. In *Internationaler motorenkongress* (pp. 93–111). http://dx.doi.org/10.1007/978-3-658-21015-1_7.

Kawamoto, R., Mochizuki, H., Moriguchi, Y., Nakano, T., Motohashi, M., Sakai, Y., & Inaba, A. (2019). Estimation of CO_2 emissions of internal combustion engine vehicle and battery electric vechicle using LCA. *MPDI Sustain.*, *11*, http://dx.doi.org/10.3390/su11092690.

König, A., Nicoletti, L., Schröder, D., Wolf, S., Waclaw, A., & Lienkamp, M. (2021). An overview of paramter and cost for battery electric vehicles. *World Electric Vehicle Journal*, *12*, 1–29. http://dx.doi.org/10.3390/wevj12010021.

Kreß, J., Morgado-Estévez, A., Perez-Peña, F., Schmidt, K., & Hebert, H. (2021). Development of single-axis wheel speed sensor HiL test bench for vehicle velocity control. In *Proc. 3rd international congress on human-computer interaction, optimization and robotic applications* (pp. 1–5). http://dx.doi.org/10.1109/HORA52670.2021.9461305.

Kreß, J., Rau, J., Hebert, H., Perez-Peña, F., Schmidt, K., & Morgado-Estévez, A. (2023). Low-cost throttle-by-wire-system architecture for two-wheeler vehicles. http://dx.doi.org/10.48550/arXiv.2304.14875, arXiv:2304.14875.

Kumar, G., Badulla, S., Nagaraju, J., Venkatesh, O., Narasimhulu, G., & Rao, V. (2023). Design and analysis of 3-way catalytic converter using CFD. *Materials Today: Proceedings*, http://dx.doi.org/10.1016/j.matpr.2023.07.215.

Kymco (2022). Kymco prospekt 2022.

Leyda, K., & Wos, P. (2012). *Internal combustion engines* (1st ed.). (pp. 71–72). Croatia: IntechOpen, http://dx.doi.org/10.5772/2806.

Lindemann, P., Steinberger, M., & Krause, T. (2014). *iTC - innovative solutions for torque converters pave the way into the future*: *vol. 20*, (pp. 280–301). Schaeffer Technologies AG & Co. KG, http://dx.doi.org/10.1007/978-3-658-06430-3_20.

Miritsch, J., Graf, H., Böck, K., & Deuschle, R. (2021). Big boxer - the engine in the new BMW R18. *MTZ Worldwide*, *82*, 48–54. http://dx.doi.org/10.1007/s38313-021-0688-1.

Peugeot Motocycle (2023). Range 50ccm.

Poschner, M., Vogt, J., Wösle, G., & Wagner, H. (2010). The new BMW s 1000 RR. *ATZ Worldwide*, *112*, 4–10. http://dx.doi.org/10.1007/BF03225247.

Smither, B., Allen, J., Ravenhill, P., Farmer, G., Grosch, P., & Demesse, E. (2011). Development of electronic throttle actuation for a 50cc 2-stroke scooter application. *SAE International*, http://dx.doi.org/10.4271/2011-32-0581.

Smither, B., McFarlane, I., Drake, T., Ravenhill, P., Allen, J., & Boak, J. (2008). Engine management system for fuel injection system specifically designed for small engines. *SAE International*, http://dx.doi.org/10.4271/2008-32-0052.

Statistical office of the European Union (2022). *Passenger mobility statistics*. Eurostat.

STMicroelectronics (2019). Data brief STM32H7B3I-DK, DB3894 rev 1.

STMicroelectronics (2021). Datasheet STM32G431x6 STM32G431x8 STM32G431xb, DS12589 rev 6.

Stoffregen, J. (2018). *Motorradtechnik* (9th ed.). (p. 43). Olching, Germany: Springer Vieweg, http://dx.doi.org/10.1007/978-3-658-07446-3.

World Energy Council (2021). *Energie für deutschland*. World Energy Council.

Zhang, Y., & Zhao, H. (2014). Investigation of combustion, performance and emission characteristics of 2-stroke and 4-stroke spark ignition and CAI/HCCI operations in a DI gasoline. *Elsevier Appl. Energy*, *130*, 244–255. http://dx.doi.org/10.1016/j.apenergy.2014.05.036.

Zhu, C., Liu, H., Tian, J., Xiao, Q., & Du, X. (2010). Experimental investigation on efficiency of the pulley-drive CVT. *International Journal of Automotive Technology*, *11*, 257–261. http://dx.doi.org/10.1007/s12239-010-0032-2.